Numer. Math. Theor. Meth. Appl.
doi: 10.4208/nmtma.2009.m9001

Vol. **3**, No. 1, pp. 23-39
February 2010

Immersed Interface Finite Element Methods for Elasticity Interface Problems with Non-Homogeneous Jump Conditions

Yan Gong[1] and Zhilin Li[2,*]

[1] *Department of Mathematics, Limestone College, Gaffney, SC 29340, USA.*
[2] *Center For Research in Scientific Computation and Department of Mathematics, North Carolina State University, Raleigh, NC 27695-8205, USA.*

Received 3 January 2009; Accepted (in revised version) 12 March 2009

Available online 30 November 2009

Abstract. In this paper, a class of new immersed interface finite element methods (IIFEM) is developed to solve elasticity interface problems with homogeneous and non-homogeneous jump conditions in two dimensions. Simple non-body-fitted meshes are used. For homogeneous jump conditions, both non-conforming and conforming basis functions are constructed in such a way that they satisfy the natural jump conditions. For non-homogeneous jump conditions, a pair of functions that satisfy the same non-homogeneous jump conditions are constructed using a level-set representation of the interface. With such a pair of functions, the discontinuities across the interface in the solution and flux are removed; and an equivalent elasticity interface problem with homogeneous jump conditions is formulated. Numerical examples are presented to demonstrate that such methods have second order convergence.

AMS subject classifications: 65N30

Key words: Immersed interface finite element methods, elasticity interface problems, singularity removal, homogeneous and non-homogeneous jump conditions, level-set function.

1. Introduction

In this paper, we consider the elasticity interface problem

$$\nabla \cdot \sigma + F = 0, \qquad \text{in } \Omega^- \cup \Omega^+, \tag{1.1}$$

where σ is the stress tensor, a 2×2 symmetric matrix, $F = (f_1,\ f_2)^T$ is a known body force. The domain Ω consists of Ω^- and Ω^+, $\Omega^- \cap \Omega^+ = \emptyset$, see Fig. 1 for an illustration. We assume that the interface $\Gamma = \overline{\Omega^-} \cap \overline{\Omega^+}$ separates Ω^- and Ω^+ is smooth enough (C^2). We also denote by $\mathbf{n}$ the unit vector normal to Γ pointing from Ω^- to Ω^+.

*Corresponding author. *Email addresses:* ygong@limestone.edu (Y. Gong), zhilin@math.ncsu.edu (Z. Li)

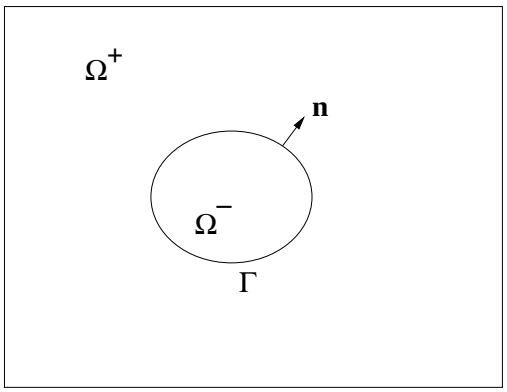

Figure 1: A diagram of the geometry of an elliptic interface problem.

For linearly elastic problems with small displacements, the relation between stress tensor and deformation is given by

$$\sigma_{ij} = \lambda(\nabla \cdot u)\,\delta_{ij} + 2\,\mu\,\varepsilon_{ij}(u), \tag{1.2}$$

where λ and μ are Lamé constants, $u = (u_1, u_2)^T$ is the displacement vector. The equations (1.1) can be written as the component form,

$$-\left\{(\lambda+2\mu)\frac{\partial^2 u_1}{\partial x_1^2} + (\lambda+\mu)\frac{\partial^2 u_2}{\partial x_1 \partial x_2} + \mu\frac{\partial^2 u_1}{\partial x_2^2}\right\} = f_1, \quad u_1\Big|_{\partial\Omega} = g_1, \tag{1.3}$$

$$-\left\{(\lambda+2\mu)\frac{\partial^2 u_2}{\partial x_2^2} + (\lambda+\mu)\frac{\partial^2 u_1}{\partial x_1 \partial x_2} + \mu\frac{\partial^2 u_2}{\partial x_1^2}\right\} = f_2, \quad u_2\Big|_{\partial\Omega} = g_2. \tag{1.4}$$

Due to the discontinuities in the coefficients, or/and source distribution along the interface Γ, the solution and flux are often discontinuous. The jump conditions across Γ can be written as

$$[u_1]_\Gamma = w_1, \tag{1.5}$$

$$[u_2]_\Gamma = w_2, \tag{1.6}$$

$$\left[\lambda\left(\frac{\partial u_1}{\partial x_1} + \frac{\partial u_2}{\partial x_2}\right)n_1 + 2\mu\frac{\partial u_1}{\partial x_1}n_1 + \mu\left(\frac{\partial u_1}{\partial x_2} + \frac{\partial u_2}{\partial x_1}\right)n_2\right]_\Gamma = q_1, \tag{1.7}$$

$$\left[\lambda\left(\frac{\partial u_1}{\partial x_1} + \frac{\partial u_2}{\partial x_2}\right)n_2 + 2\mu\frac{\partial u_2}{\partial x_2}n_2 + \mu\left(\frac{\partial u_1}{\partial x_2} + \frac{\partial u_2}{\partial x_1}\right)n_1\right]_\Gamma = q_2. \tag{1.8}$$

The jump conditions are called *natural* if

$$w_1 = w_2 = q_1 = q_2 = 0.$$

Elastic interface problems (1.3)-(1.4) with such jump conditions arise in many areas, for example, the epitaxial growth of thin films [2,6].

To solve the interface problem, first we need to generate a mesh. One approach is to use a body fitted mesh coupled with a finite element discretization, see for example, [1,5,7,8,11,17] for scalar elliptic partial differential equations (PDEs). Recently, Cartesian meshes have become popular especially for moving interface problems to overcome the cost in the grid generation at every or every other time steps.

Finite difference methods are proposed in [18,19] with non-homogeneous jump conditions. While second order accuracy was achieved, the condition number of the discrete system is quite large especially in the nearly incompressible case (λ is large) compared with that obtained from finite element formulations. In [18,19], a first order immersed interface finite element method (IIFEM) was proposed using Cartesian meshes for the elasticity problem with *homogeneous* jump conditions. In general, the discretization using a finite element discretization has better conditioned system of equations compared with that obtained from a finite difference method. The Soblev space theory provides strong theoretical foundations for convergence analysis for finite element methods.

In [10], an immersed-interface finite element method was developed for *scalar* elliptic interface problems with *non-homogeneous* jump conditions. In this paper, we propose immersed-interface finite element methods for the elastic system with homogeneous and non-homogeneous jump conditions. In some sense, this paper is a non-trivial extension to the work in [10]. While the idea is similar, the discussion and implementation are substantially more difficult as we can see later in this paper.

The basic idea of our immersed-interface finite method for homogeneous jump conditions is to incorporate the jump conditions in constructing basis functions. In a finite difference immersed interface method, the jump conditions are enforced through finite difference equations at grid points near or on the interface. In the immersed interface finite element methods, the jump conditions are enforced through the construction of special finite-element basis functions that satisfy the homogeneous jump conditions ($w_1 = w_2 = q_1 = q_2 = 0$). Clearly, such basis functions depend on the interface location and the physical parameters.

To deal with non-homogeneous jump conditions, we construct a known functions with the same jump conditions via a level set function whose zero level set is the interface Γ. Through the known function, we transform the original elastic interface problem to a new one with homogeneous jump conditions. In implementation, the process is equivalent to moving the non-homogeneous jump conditions to the right hand sides.

The paper is organized as follows. In Section 2, we review the immersed interface non-conforming finite element method for elasticity interface problems. In Section 3, we describe the immersed interface finite element methods for elasticity interface problems with homogeneous jump conditions and present a numerical example. In Section 4, we describe the immersed-interface finite-element methods for elasticity interface problems with non-homogeneous jump conditions and present some numerical results.

2. Review of the non-conforming immersed interface finite element space

The weak formulation of the elasticity problem (1.3)-(1.4) with homogeneous jump conditions ($w_1 = w_2 = q_1 = q_2 = 0$) is,

$$a(u,v) = L(v), \qquad \forall v \in \{H_0^1(\Omega)\}^2, \tag{2.1}$$

where

$$a(u,v) = \int_\Omega \left\{ \lambda \left(\frac{\partial u_1}{\partial x_1} + \frac{\partial u_2}{\partial x_2} \right) \left(\frac{\partial v_1}{\partial x_1} + \frac{\partial v_2}{\partial x_2} \right) + 2\mu \left(\frac{\partial u_1}{\partial x_1}\frac{\partial v_1}{\partial x_1} + \frac{\partial u_2}{\partial x_2}\frac{\partial v_2}{\partial x_2} \right) \right.$$
$$\left. + \mu \left(\frac{\partial u_1}{\partial x_2} + \frac{\partial u_2}{\partial x_1} \right) \left(\frac{\partial v_1}{\partial x_2} + \frac{\partial v_2}{\partial x_1} \right) \right\} dx,$$

see, for example, [4] for a reference.

Let $\mathscr{T}_h$ be a finite-element mesh with mesh size h that covers $\overline{\Omega}$. We assume that the elements in $\mathscr{T}_h$ are all triangles. For simplicity, we shall assume that Ω is a convex polygonal domain and the mesh covers $\overline{\Omega}$ exactly. Standard finite element techniques can be applied to treat a curved boundary. In practice the computational domain Ω can often be chosen as a rectangular domain with sides parallel to the coordinate axes; and the finite-element mesh can be uniform.

We call an element $T \in \mathscr{T}_h$ an *interface element* if $\Gamma \cap \operatorname{int} T \neq \emptyset$. Note that an element is a non-interface element, if one of its edges is part of the interface. We assume for any interface element $T \in \mathscr{T}_h$, the set $\Gamma \cap \partial T$ consists of exactly two points that are on different edges of T.

We define an immersed-interface finite-element space V_h with respect to the mesh $\mathscr{T}_h$ to be a finitely-dimensional subspace of $L^2(\Omega)$ that consists of all the linear combinations of the corresponding basis functions $\phi_1, \cdots, \phi_N$ for some integer $N \geq 1$:

$$V_h = \operatorname{span}\{v_1, v_2, \cdots, v_N\}, \tag{2.2}$$

where v_i are vector functions of two dimensions. The basis functions are the usual finite-element basis functions on a non-interface element, in which the set of shape functions are given by

$$\phi^e = \begin{pmatrix} \phi_1 & 0 & \phi_2 & 0 & \phi_3 & 0 \\ 0 & \phi_1 & 0 & \phi_2 & 0 & \phi_3 \end{pmatrix}, \tag{2.3}$$

where ϕ_i, $i = 1, 2, 3$, are the standard shape functions with $\phi_i(x_j) = \delta_{ij}$, see for example, [3] for the details.

On an interface element, the basis functions are also chosen as piecewise polynomials that are determined by the element and the interface Γ. All the basis functions satisfy the homogeneous jump conditions for both of the function and flux. Moreover, there exists an interpolation operator from some functional space to V_h that enjoys the usual approximation properties.

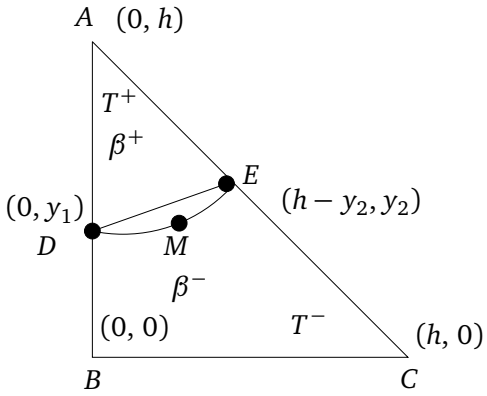

Figure 2: A typical interface element $T = \triangle ABC$. The arc DME is the part of the interface Γ in T. It is approximated by the line segment $\overline{DE}$. $T^+ = \triangle ADE$, $T^- = T - T^+$, and T_r is the region enclosed by the $\overline{DE}$ and the arc DME.

At an interface triangle, see Fig. 2 for a typical example, we consider how to construct a piecewise linear function $\phi(x_1, x_2) = [\phi_1(x_1, x_2),\ \psi_1(x, y)]^T$ given its values at the three vertices. Let

$$\phi_1(x) = \begin{cases} c_{\phi_1}^{(1)} + c_{\phi_1}^{(2)} x_1 + c_{\phi_1}^{(3)} x_2, & \text{if } x = (x_1, x_2) \in T^+, \\ c_{\phi_1}^{(4)} + c_{\phi_1}^{(5)} x_1 + c_{\phi_1}^{(6)} x_2, & \text{if } x = (x_1, x_2) \in T^-, \end{cases} \tag{2.4}$$

$$\psi_1(x) = \begin{cases} c_{\psi_1}^{(1)} + c_{\psi_1}^{(2)} x_1 + c_{\psi_1}^{(3)} x_2, & \text{if } x = (x_1, x_2) \in T^+, \\ c_{\psi_1}^{(4)} + c_{\psi_1}^{(5)} x_1 + c_{\psi_1}^{(6)} x_2, & \text{if } x = (x_1, x_2) \in T^-. \end{cases} \tag{2.5}$$

There are twelve unknown coefficients. There are chosen to satisfy the values at three vertices, which gives six equations; the continuity condition at D and E, which gives four equations; the flux jump conditions (1.7)-(1.8), which provides additional two constraints. Thus the number of unknowns is the same as the number of equations. The coefficient matrix is non-singular for physically meaningful parameters, we refer the reader to [9] for more details.

Remark 2.1. The idea of constructing the non-conforming basis functions is the same as for the scaler elliptic interface problems described in [10]. However, we can not construct the basis functions for the system using the dimension by dimension approach due to the coupling of the flux jump condition (1.8).

Note that from the construction process, we can see that if the components of the solution are piecewise linear functions, then the constructed interpolation function using the nodal values would be exact except for a small mis-matched regions whose area is at most $\mathcal{O}(h^3)$, where h is the uniform mesh size. Therefore, the constructed interpolation

function using the constructed finite element basis functions is second order accurate in the L^∞ norm. On the other hand, while the basis functions are continuous on each element (triangle), they may not match with other pieces defined on neighboring triangles. So the finite element space is a non-conforming one. The convergence rate is observed between first order and second order in the L^∞ norm.

3. A conforming finite element space

In this section, we show how to construct a conforming linear finite element space. The basis functions associated with interface elements are still piecewise linear and globally continuous. The method extended the idea for scale interface problems in [10], the conforming finite element space can be regarded as a perturbation to the non-conforming one.

In order to maintain the continuity in the basis functions, we extend the previously defined basis functions at an interface element to one more triangle along the interface (cf. Fig. 3 (b)). We require that the local basis functions in two adjacent interface elements, such as ΔABC and ΔAFB, take the same value at the interface point (D) on their common edge.

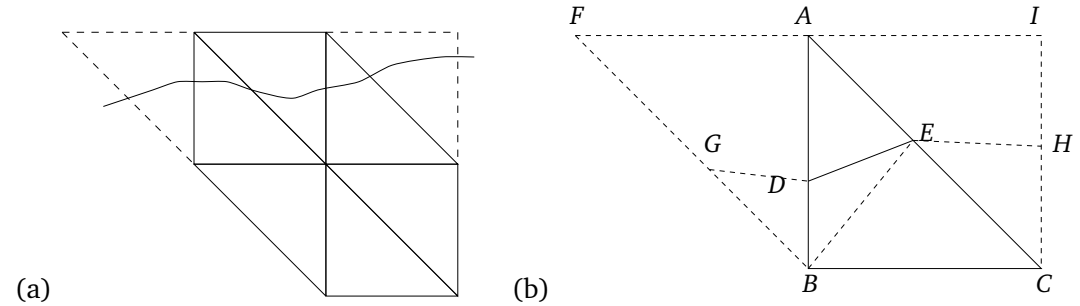

Figure 3: (a) The support of a local basis function. (b) A diagram for the construction of a local basis function on $\triangle ABC$.

For an interface element $T = \Delta ABC \in \mathcal{T}_h$, see Fig. 3 for an illustration, we denote the set of basis functions as

$$\phi^e = \begin{pmatrix} \bar{\phi}_1 & \bar{\phi}_2 & \bar{\phi}_3 & \bar{\phi}_4 & \bar{\phi}_5 & \bar{\phi}_6 & \bar{\phi}_7 & \bar{\phi}_8 & \bar{\phi}_9 & \bar{\phi}_{10} \\ \psi_1 & \psi_2 & \psi_3 & \psi_4 & \psi_5 & \psi_6 & \psi_7 & \psi_8 & \psi_9 & \psi_{10} \end{pmatrix}. \tag{3.1}$$

We construct $\bar{\phi}_i$ and ψ_i, $i = 1, 2, \cdots, 10$, by assigning their values (zero or unity) at the vertices A, B, C, F, and I, respectively. This construction process can be summarized in the following steps:

P1. Use the values at the nodes A, B, C, F, and I to construct the three sets of *non-conforming* finite element basis functions on the elements ΔABC, ΔAFB, and ΔACI, respectively, as explained in Section 2;

P2. Set the value at D as the average of the values at D of the non-conforming basis functions defined on ΔABC and ΔAFB constructed in **P1**;

P3. Similarly, set the value at E as the average of values at E of the non-conforming basis functions defined on the elements ΔABC and ΔACI constructed in **P1**;

P4. Set the values at the points A, B and C exactly the same as those from the non-conforming finite-element basis function on ΔABC:

$$\phi^e(B) = \begin{pmatrix} 1 & 0 & 0 & 0 & 0 & 0 & 0 & 0 & 0 & 0 \\ 0 & 1 & 0 & 0 & 0 & 0 & 0 & 0 & 0 & 0 \end{pmatrix},$$

$$\phi^e(C) = \begin{pmatrix} 0 & 0 & 1 & 0 & 0 & 0 & 0 & 0 & 0 & 0 \\ 0 & 0 & 0 & 1 & 0 & 0 & 0 & 0 & 0 & 0 \end{pmatrix},$$

$$\phi^e(A) = \begin{pmatrix} 0 & 0 & 0 & 0 & 1 & 0 & 0 & 0 & 0 & 0 \\ 0 & 0 & 0 & 0 & 0 & 1 & 0 & 0 & 0 & 0 \end{pmatrix};$$

P5. Partition the element ΔABC into three sub-triangles by an auxiliary line, say line segment $\overline{BE}$, or $\overline{DC}$. We choose the auxiliary line in such a way that at least one of angles (or complimentary angle if the angle is more than $\pi/4$) is bigger than or equal to $\pi/2$, see [14] for more explanations;

P6. Define the basis functions $\bar{\phi}_i$ and ψ_i, $i = 1, 2, \cdots, 10$, to be the piecewise linear function in the three sub-triangles.

Remark 3.1. Note that if all the coefficients are continuous, then the non-zero basis functions are the standard piecewise linear basis functions. For coefficients with jumps across the interface Γ, we can think that the compact support region of a global basis function has been extended from interface element to one or two triangles along the interface to keep the continuity of the basis function.

3.1. A numerical example for the conforming IIFEM with homogeneous jump conditions

We consider the problem (1.4)-(1.6) with $\Omega = (-1,1) \times (-1,1)$, Γ being the circle centered at point $(0,0)$ with radius $R = 0.5$, and $\lambda^- = \mu^- = 1$, and $\lambda^+ = \mu^+ = 100$. The body force term $F = (f_1, f_2)$ and the Dirichlet boundary condition $G = (g_1, g_2)$ are from the exact solution $u = (u_1, u_2)$,

$$u_1(x_1, x_2) = u_2(x_1, x_2) = \begin{cases} (x_1^2 + x_2^2), & \text{if } r \le R, \\ \dfrac{(x_1^2 + x_2^2)}{100} + \left(1 - \dfrac{1}{100}\right) R^2, & \text{otherwise,} \end{cases}$$

where $r = \sqrt{x_1^2 + x_2^2}$. The exact solution satisfies the homogeneous jump conditions ($w_1 = w_2 = q_1 = q_2 = 0$).

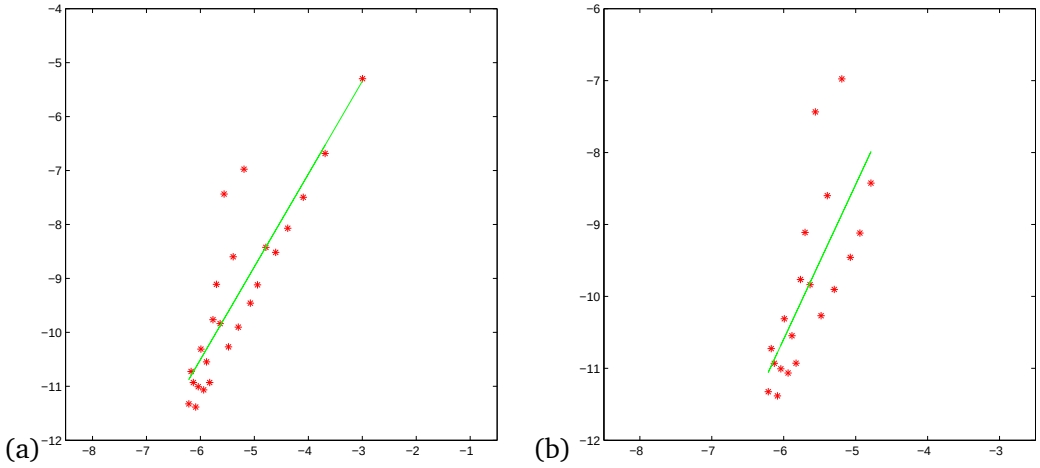

Figure 4: The linear regression analysis of $\|u-u^I\|_{L^\infty}$ in log-log scale of the interpolation error using the conforming linear IIFE space. (a), the mesh is varying according to $N = 20+20k$, $k = 0,1,\cdots,24$, the slope (convergence order) is 1.7192; (b), $N = 120+20k$, $k = 0,1,\cdots,19$, the slope is 2.1479.

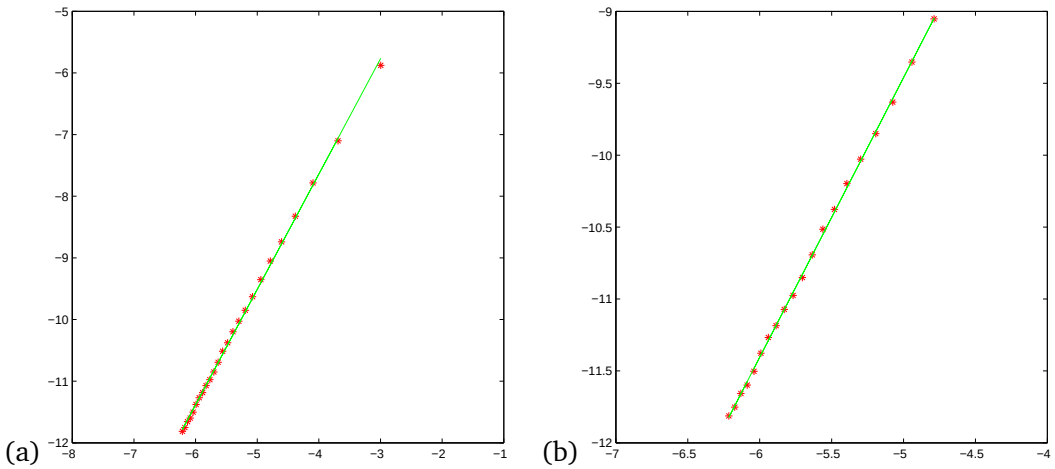

Figure 5: The linear regression analysis of $(u-u^h)$ in the L^∞ norm in log-log scale by using the conforming, linear, immersed interface finite element space. (a), the mesh is varying according to $N = 20+20k$, $k = 0,1,\cdots,24$, the slope (convergence order) is 1.8706; (b), $N = 120+20k$, $k = 0,1,\cdots,19$, the slope is 1.9443.

For this problem, even though the solution is piecewise quadratic, we can not get the exact solution due to the approximation of Γ using piecewise line segments. But we show that the interpolation error, and the global error of the finite element solution both have asymptotic second order convergence in the L^∞ norm.

With fixed Cartesian meshes, the L^∞ errors usually do not decrease monotonically because there is no fixed patten between the underlying mesh and the interface as we refine the mesh. Thus it is more appropriate to find average convergence order using

linear regression analysis, see for example, [12, 13] for more details. In Fig. 4, we show the grid refinement results in log-log scale for the error of the interpolation function u^I. In Fig. 4 (a), the meshes are taken as $N = 20 + 20k$, $k = 0, 1, \cdots, 24$, the slope of the fitted line (convergence order) is 1.7192. For the coarser grid, the error in representing the interface has some effect on the convergence order. In Fig. 4 (b), we start with a finer mesh, $N = 120 + 20k$, $k = 0, 1, \cdots, 19$, the slope of the fitted line is 2.1479 which gives more accurate account about the convergence order.

In Fig. 5, we show the grid refinement analysis for the finite element solution by plotting and fitting the error $\|u - u^h\|_{L^\infty}$. The convergence order is 1.8706 with the mesh varying according to $N = 120 + 20k$, $k = 0, 1, \cdots, 19$ in Fig. 5 (a); and 1.9443 with the mesh varying according to $N = 120 + 20k$, $k = 0, 1, \cdots, 24$ in Fig. 5 (b).

4. IIFEM for elasticity system with non-homogeneous jump conditions

In theory, the conforming IIFEM only works for homogeneous jump conditions, that is, $w_1 = w_2 \equiv 0$ and $q_1 = q_2 \equiv 0$. It is possible to treat non-homogeneous jump in the fluxes ($q_1 \neq 0$ and $q_2 \neq 0$) as line integrals. But the convergence order in the L^∞ norm will likely be deteriorated. It is almost impossible to have second order finite element method using the basis constructed in previous section since any linear combination of the basis functions would satisfy the homogeneous jump conditions.

One efficient way of overcoming this difficulty is the singularity removal technique first developed for the scalar problems [10]. The idea is to construct a known function with the same jump conditions to transform the original problem to a new one with homogeneous jump conditions via a level set representation of the interface Γ.

Let $\varphi(x_1, x_2)$ be a Lipschitz continuous function whose zero level set is the interface

$$\Gamma = \{ (x_1, x_2),\ \varphi(x_1, x_2) = 0 \}.$$

A commonly used one is the signed distance function, which is a smooth function (C^2) in the neighborhood of the interface if the interface is smooth (C^2). We refer the readers to [15,16] about the level set method. Note that, given an fixed interface, one can generate the signed distance function numerically.

In the source singularity removal technique, we extend the jump conditions along the normal line in each direction. We denote these extension as $w_i^e(x_1, x_2)$ and $q_i^e(x_1, x_2)$, $i = 1, 2$. Note that the extensions are two dimensional functions at least in a neighborhood of the interface and they are constants along the normal lines of the interface. The theoretical justification of the extension was established in [10], which we repeat in the following lemma,

Lemma 4.1. *Let $\rho > 0$ be small enough. Then, for any $x \in N(\Gamma, \rho)$, there exists a unique $x^* \in \Gamma$ such that*

$$|x - x^*| = dist(x, \Gamma). \tag{4.1}$$

Moreover,

$$\frac{x-x^*}{|x-x^*|}=\begin{cases}-n(x^*) & \text{if } x\in\Omega^-,\\ +n(x^*) & \text{if } x\in\Omega^+,\end{cases} \tag{4.2}$$

where $n(x^*)$ is the unit normal to Γ at x^*, pointing from Ω^- to Ω^+.

We define $\tilde{u}=(\tilde{u}_1,\tilde{u}_2)$ as

$$\tilde{u}_1=w_1^e(x)+J_1^e(x)\frac{\varphi(x)}{|\nabla\varphi(x)|},\qquad \forall x\in\Omega, \tag{4.3a}$$

$$\tilde{u}_2=w_2^e(x)+J_2^e(x)\frac{\varphi(x)}{|\nabla\varphi(x)|},\qquad \forall x\in\Omega, \tag{4.3b}$$

where $J_1^e:\Omega\to\mathbb{R}$, $J_2^e:\Omega\to\mathbb{R}$ are the extensions of $J_1:\Gamma\to\mathbb{R}$, $J_2:\Gamma\to\mathbb{R}$.

Note that $J_1:\Gamma\to\mathbb{R}$, $J_2:\Gamma\to\mathbb{R}$, $J_1^e:\Omega\to\mathbb{R}$ and $J_2^e:\Omega\to\mathbb{R}$ are *unknown functions* and will be determined later in this section. They satisfy the following conditions:

- J_1^e and J_2^e are smooth on $\overline{\Omega}$, J_1 and J_2 are smooth on Γ;
- $J_1^e(x)=J_1(x^*)$ and $J_2^e(x)=J_2(x^*)$ for any $x\in N(\Gamma,\rho)$, where x^* is defined as in Lemma 4.1;
- $J_1^e(x)=0$ and $J_2^e(x)=0$ for any $x\in\Omega\setminus N(\Gamma,\rho)$.

We then define $\hat{u}=(\hat{u}_1,\hat{u}_2)$ as:

$$\hat{u}_1=\chi_{\Omega^+}(x)\tilde{u}_1(x),\qquad \forall x\in\Omega, \tag{4.4a}$$

$$\hat{u}_2=\chi_{\Omega^+}(x)\tilde{u}_2(x),\qquad \forall x\in\Omega, \tag{4.4b}$$

where χ_{Ω^+} is the characteristic of function of Ω^+. The function $\hat{u}=(\hat{u}_1,\hat{u}_2)$ has the following properties:

- $\hat{u}_1^+$, $\hat{u}_1^-$, $\hat{u}_2^+$, and $\hat{u}_2^-$ are smooth on Ω^- and Ω^+, respectively;
- $\hat{u}_1=g_1$ and $\hat{u}_2=g_2$ on $\partial\Omega$;
- $\hat{u}=(\hat{u}_1,\hat{u}_2)$ has the same non-homogeneous jump conditions across the interface Γ as $u=(u_1,u_2)$,

$$\left[\hat{u}_1\right]_\Gamma=w_1, \tag{4.5a}$$

$$\left[\hat{u}_2\right]_\Gamma=w_2, \tag{4.5b}$$

$$\left[\lambda\left(\frac{\partial\hat{u}_1}{\partial x_1}+\frac{\partial\hat{u}_2}{\partial x_2}\right)n_1+2\mu\frac{\partial\hat{u}_1}{\partial x_1}n_1+\mu\left(\frac{\partial\hat{u}_1}{\partial x_2}+\frac{\partial\hat{u}_2}{\partial x_1}\right)n_2\right]_\Gamma=q_1, \tag{4.5c}$$

$$\left[\lambda\left(\frac{\partial\hat{u}_1}{\partial x_1}+\frac{\partial\hat{u}_2}{\partial x_2}\right)n_2+2\mu\frac{\partial\hat{u}_2}{\partial x_2}n_2+\mu\left(\frac{\partial\hat{u}_1}{\partial x_2}+\frac{\partial\hat{u}_2}{\partial x_1}\right)n_1\right]_\Gamma=q_2. \tag{4.5d}$$

Now we discuss how to find the functions J_1 and J_2 in the following procedure.

• Find the partial derivatives of $\tilde{u}_1$ and $\tilde{u}_2$. Note that $\varphi(x) = 0$ on the interface Γ, we have

$$\frac{\partial J_1^e}{\partial x_1}\left(\frac{\varphi}{|\nabla\varphi|}\right) = \frac{\partial J_1^e}{\partial x_2}\left(\frac{\varphi}{|\nabla\varphi|}\right) = \frac{\partial J_2^e}{\partial x_1}\left(\frac{\varphi}{|\nabla\varphi|}\right) = \frac{\partial J_2^e}{\partial x_2}\left(\frac{\varphi}{|\nabla\varphi|}\right) = 0,$$

and

$$\left.\frac{\partial \tilde{u}_1}{\partial x_1}\right|_\Gamma = \frac{\partial w_1^e}{\partial x_1} + J_1\frac{\partial}{\partial x_1}\left(\frac{\varphi(x)}{|\nabla\varphi(x)|}\right), \tag{4.6a}$$

$$\left.\frac{\partial \tilde{u}_1}{\partial x_2}\right|_\Gamma = \frac{\partial w_1^e}{\partial x_2} + J_1\frac{\partial}{\partial x_2}\left(\frac{\varphi(x)}{|\nabla\varphi(x)|}\right), \tag{4.6b}$$

$$\left.\frac{\partial \tilde{u}_2}{\partial x_1}\right|_\Gamma = \frac{\partial w_2^e}{\partial x_1} + J_2\frac{\partial}{\partial x_1}\left(\frac{\varphi(x)}{|\nabla\varphi(x)|}\right), \tag{4.6c}$$

$$\left.\frac{\partial \tilde{u}_2}{\partial x_2}\right|_\Gamma = \frac{\partial w_2^e}{\partial x_2} + J_2\frac{\partial}{\partial x_2}\left(\frac{\varphi(x)}{|\nabla\varphi(x)|}\right). \tag{4.6d}$$

• Obtain the following equations after we plug (4.4) into (4.5c)-(4.5d),

$$\lambda^+ n_1\left(\frac{\partial \tilde{u}_1}{\partial x_1} + \frac{\partial \tilde{u}_2}{\partial x_2}\right)\Big|_\Gamma + 2\mu^+ n_1\left.\frac{\partial \tilde{u}_1}{\partial x_1}\right|_\Gamma + \mu^+ n_2\left(\frac{\partial \tilde{u}_1}{\partial x_2} + \frac{\partial \tilde{u}_2}{\partial x_1}\right)\Big|_\Gamma = q_1, \tag{4.7a}$$

$$\lambda^+ n_2\left(\frac{\partial \tilde{u}_1}{\partial x_1} + \frac{\partial \tilde{u}_2}{\partial x_2}\right)\Big|_\Gamma + 2\mu^+ n_2\left.\frac{\partial \tilde{u}_2}{\partial x_2}\right|_\Gamma + \mu^+ n_1\left(\frac{\partial \tilde{u}_1}{\partial x_2} + \frac{\partial \tilde{u}_2}{\partial x_1}\right)\Big|_\Gamma = q_2. \tag{4.7b}$$

• Set equations for J_1, J_2 after we plug (4.6) into (4.7) and rearrange terms to get

$$a_{11}^J J_1 + a_{12}^J J_2 = b_1^J, \tag{4.8a}$$

$$a_{21}^J J_1 + a_{22}^J J_2 = b_2^J, \tag{4.8b}$$

where

$$\begin{aligned}
a_{11}^J &= (\lambda^+ + 2\mu^+)n_1\frac{\partial}{\partial x_1}\left(\frac{\varphi(x)}{|\nabla\varphi(x)|}\right) + \mu^+ n_2\frac{\partial}{\partial x_2}\left(\frac{\varphi(x)}{|\nabla\varphi(x)|}\right),\\
a_{12}^J &= \lambda^+ n_1\frac{\partial}{\partial x_2}\left(\frac{\varphi(x)}{|\nabla\varphi(x)|}\right) + \mu^+ n_2\frac{\partial}{\partial x_1}\left(\frac{\varphi(x)}{|\nabla\varphi(x)|}\right),\\
a_{21}^J &= \mu^+ n_1\frac{\partial}{\partial x_2}\left(\frac{\varphi(x)}{|\nabla\varphi(x)|}\right) + \lambda^+ n_2\frac{\partial}{\partial x_1}\left(\frac{\varphi(x)}{|\nabla\varphi(x)|}\right),\\
a_{22}^J &= \mu^+ n_1\frac{\partial}{\partial x_1}\left(\frac{\varphi(x)}{|\nabla\varphi(x)|}\right) + (\lambda^+ + 2\mu^+)n_2\frac{\partial}{\partial x_2}\left(\frac{\varphi(x)}{|\nabla\varphi(x)|}\right),
\end{aligned}$$

and

$$\begin{aligned}
b_1^J &= q_1 - (\lambda^+ + 2\mu^+)n_1\frac{\partial w_1^e}{\partial x_1} - \lambda^+ n_1\frac{\partial w_2^e}{\partial x_2} - \mu^+ n_2\frac{\partial w_1^e}{\partial x_2} - \mu^+ n_2\frac{\partial w_2^e}{\partial x_1},\\
b_2^J &= q_2 - (\lambda^+ + 2\mu^+)n_2\frac{\partial w_2^e}{\partial x_2} - \lambda^+ n_2\frac{\partial w_1^e}{\partial x_1} - \mu^+ n_1\frac{\partial w_1^e}{\partial x_2} - \mu^+ n_1\frac{\partial w_2^e}{\partial x_1}.
\end{aligned}$$

• Let A^J to be a 2×2 matrix and b^J, x^J to be 2×1 vectors, we have

$$A^J=\begin{pmatrix} a_{11}^J & a_{12}^J \\ a_{21}^J & a_{22}^J \end{pmatrix},\qquad x^J=\begin{pmatrix} J_1 \\ J_2 \end{pmatrix},\qquad b^J=\begin{pmatrix} b_1^J \\ b_2^J \end{pmatrix}. \tag{4.9}$$

Consequently, (4.8) can be written as

$$A^J x^J = b^J.$$

Thus J_1 and J_2 can be solved from $x^J=(A^J)^{-1}b^J$.

4.1. Computing the modified load vector

If we set $u=u^H+\hat{u}$, then u^H satisfies the elasticity equations with homogeneous jump conditions. We can then use the IIFEM method described in the previous sections to solve for u^H, which also leads to u since $\hat{u}$ is a known function. In practice, we can get the solution directly after some manipulations.

Note that, by plugging $u=u^H+\hat{u}$ into the elasticity equations, we can get

$$\nabla\cdot\sigma^H+F^H=0, \tag{4.10}$$

which can be written as

$$-\left\{(\lambda+2\mu)\frac{\partial^2 u_1^H}{\partial x_1^2}+(\lambda+\mu)\frac{\partial^2 u_2^H}{\partial x_1\partial x_2}+\mu\frac{\partial^2 u_1^H}{\partial x_2^2}\right\}=f_1^H, \tag{4.11a}$$

$$-\left\{(\lambda+2\mu)\frac{\partial^2 u_2^H}{\partial x_2^2}+(\lambda+\mu)\frac{\partial^2 u_1^H}{\partial x_1\partial x_2}+\mu\frac{\partial^2 u_2^H}{\partial x_1^2}\right\}=f_2^H, \tag{4.11b}$$

where the body force $F^H=(f_1^H,f_2^H)$ associated with u^H is given by

$$f_1^H=f_1+\left\{(\lambda+2\mu)\frac{\partial^2\hat{u}_1}{\partial x_1^2}+(\lambda+\mu)\frac{\partial^2\hat{u}_2}{\partial x_1\partial x_2}+\mu\frac{\partial^2\hat{u}_1}{\partial x_2^2}\right\}, \tag{4.12a}$$

$$f_2^H=f_2+\left\{(\lambda+2\mu)\frac{\partial^2\hat{u}_2}{\partial x_2^2}+(\lambda+\mu)\frac{\partial^2\hat{u}_1}{\partial x_1\partial x_2}+\mu\frac{\partial^2\hat{u}_2}{\partial x_1^2}\right\}. \tag{4.12b}$$

The weak form of the interface problem for u^H is

$$\begin{aligned} a(u^H,v)=&\int_\Omega\left\{(\lambda+2\mu)\frac{\partial u_1^H}{\partial x_1}\frac{\partial v_1}{\partial x_1}+(\lambda+2\mu)\frac{\partial u_2^H}{\partial x_2}\frac{\partial v_2}{\partial x_2}+\mu\frac{\partial u_1^H}{\partial x_2}\frac{\partial v_1}{\partial x_2}+\mu\frac{\partial u_2^H}{\partial x_1}\frac{\partial v_2}{\partial x_1}\right.\\ &\left.+\lambda\frac{\partial u_1^H}{\partial x_1}\frac{\partial v_2}{\partial x_2}+\lambda\frac{\partial u_2^H}{\partial x_2}\frac{\partial v_1}{\partial x_1}+\mu\frac{\partial u_1^H}{\partial x_2}\frac{\partial v_2}{\partial x_1}+\mu\frac{\partial u_2^H}{\partial x_1}\frac{\partial v_1}{\partial x_2}\right\}dx\\ =L(v)=&\int_\Omega\left(f_1^H v_1+f_2^H v_2\right)dx,\qquad \forall v\in\{H_0^1(\Omega)\}^2. \end{aligned}$$

Let the resulting linear system of u^H be $AU^H = F^{H_L}$ using the conforming immersed interface finite element method. We use F^{H_L} to represent the load vector associated with u^H to avoid the confusion with the body force F^H associated with u^H. The entries of A and F^{H_L} are

$$a_{ij} = \int_\Omega \left\{ (\lambda+2\mu)\frac{\partial \phi_j}{\partial x_1}\frac{\partial \phi_i}{\partial x_1} + (\lambda+2\mu)\frac{\partial \psi_j}{\partial x_2}\frac{\partial \psi_i}{\partial x_2} + \mu\frac{\partial \phi_j}{\partial x_2}\frac{\partial \phi_i}{\partial x_2} + \mu\frac{\partial \psi_j}{\partial x_1}\frac{\partial \psi_i}{\partial x_1} \right.$$
$$\left. + \lambda\frac{\partial \phi_j}{\partial x_1}\frac{\partial \psi_i}{\partial x_2} + \lambda\frac{\partial \psi_j}{\partial x_2}\frac{\partial \phi_i}{\partial x_1} + \mu\frac{\partial \phi_j}{\partial x_2}\frac{\partial \psi_i}{\partial x_1} + \mu\frac{\partial \psi_j}{\partial x_1}\frac{\partial \phi_i}{\partial x_2} \right\} dx,$$

$$F_i^{H_L} = \int_\Omega \left(f_1^H \phi_i + f_2^H \psi_i \right) dx.$$

We also define U, $\hat{U}$ and U^H to be $2N \times 1$ vectors,

$$U = (u_1^{(1)}, u_2^{(1)}, u_1^{(2)}, u_2^{(2)}, \cdots, u_1^{(i)}, u_2^{(i)}, \cdots, u_1^{(N)}, u_2^{(N)})^T, \tag{4.13a}$$

$$\hat{U} = (\hat{u}_1^{(1)}, \hat{u}_2^{(1)}, \hat{u}_1^{(2)}, \hat{u}_2^{(2)}, \cdots, \hat{u}_1^{(i)}, \hat{u}_2^{(i)}, \cdots, \hat{u}_1^{(N)}, \hat{u}_2^{(N)})^T, \tag{4.13b}$$

$$U^H = \Big((u_1^H)^{(1)}, (u_2^H)^{(1)}, (u_1^H)^{(2)}, (u_2^H)^{(2)}, \cdots, (u_1^H)^{(i)}, (u_2^H)^{(i)}, \cdots, (u_1^H)^{(N)}, (u_2^H)^{(N)} \Big)^T, \tag{4.13c}$$

where $(u_1^{(i)}, u_2^{(i)})$, $((u_1^H)^{(i)}, (u_2^H)^{(i)})$ are the finite element solutions of u, and u^H at the i^{th} node (N_i), $i = 1, \cdots, N$, and $(\hat{u}_1^{(i)}, \hat{u}_2^{(i)})$ are the exact values of the function $\hat{u}$ at i^{th} node (N_i), $i = 1, \cdots, N$. By $U = U^H + \hat{U}$, we have

$$AU = A(U^H + \hat{U}) = AU^H + A\hat{U} = F^{H_L} + A\hat{U} = F.$$

Note that, the coefficient matrix A is the same as in that of the same problem with homogeneous jump conditions. We only need to adjust some entries of the load vector F based on F^{H_L}. The computation of the load vector is summarized below:

$$F_i = \begin{cases} \displaystyle\int_\Omega \left(f_1 \phi_i + f_2 \psi_i \right) dx, & \text{if } \Omega^s(\phi_i, \psi_i) \cap \Gamma = \emptyset, \\ \displaystyle\int_\Omega \left(f_1 \phi_i + f_2 \psi_i \right) dx & \\ \quad + \displaystyle\int_\Omega \left\{ (\lambda+2\mu)\frac{\partial^2 \hat{u}_1}{\partial x_1^2} + (\lambda+\mu)\frac{\partial^2 \hat{u}_2}{\partial x_1 \partial x_2} + \mu\frac{\partial^2 \hat{u}_1}{\partial x_2^2} \right\} \phi_i \, dx & \\ \quad + \displaystyle\int_\Omega \left\{ (\lambda+2\mu)\frac{\partial^2 \hat{u}_2}{\partial x_2^2} + (\lambda+\mu)\frac{\partial^2 \hat{u}_1}{\partial x_1 \partial x_2} + \mu\frac{\partial^2 \hat{u}_2}{\partial x_1^2} \right\} \psi_i \, dx & \\ \quad + \displaystyle\sum_{j=1}^{2N} a_{ij} \hat{U}_j, & \text{otherwise}, \end{cases} \tag{4.14}$$

where $\Omega^s(\phi_i, \psi_i)$ is the non-zero support region of ϕ_i and ψ_i, $i = 1, \cdots, N$.

4.2. A numerical example with non-homogeneous jump conditions

We consider the problem (1.3)-(1.6) with $\Omega = (-1,1)\times(-1,1)$. The interface Γ is a circle centered at the origin with radius $R = 0.5$. The parameters are $\lambda^- = \mu^- = 1$ and $\lambda^+ = \mu^+ = 100$. The exact solution $u = (u_1, u_2)$:

$$u_1 = \begin{cases} r^2, & \text{if } r \le R, \\ \dfrac{1}{b}\left(r^2 + \log(r)\right), & \text{otherwise,} \end{cases}$$

$$u_2 = \begin{cases} r^2, & \text{if } r \le R, \\ \dfrac{1}{b}\left(r^2 + \sin(x_1)\cos(x_2),\right), & \text{otherwise,} \end{cases}$$

where $r = \sqrt{x_1^2 + x_2^2}$ and $b = \max\{(\lambda^+/\lambda^-),(\mu^+/\mu^-)\}$. The exact solutions are non-linear with non-homogeneous jump conditions both in the solutions and the fluxes.

In Fig. 6, we show the results of a grid refinement analysis for the errors $\|u - u^h\|_{L^\infty}$ using the conforming IIFE method and the singularity removal technique. The convergence order from the sample meshes ranging from 20 to 500 with 20 increment is 1.9095, see Fig. 6 (a). When cutting the results from coarse meshes, the convergence order increases to 2.0222, see Fig. 6 (b). It shows clearly that the method has second order accuracy.

4.3. An example with discontinuous Lamé constants and non-homogeneous jump conditions

We consider the problem with $\Omega = (-1,1)\times(-1,1)$, Γ being the circle centered at point $(0,0)$ with radius $R = 0.5$, and

$$\lambda = \begin{cases} \lambda^- = 3 & \text{if } r \le R, \\ \lambda^+ = 30 & \text{otherwise,} \end{cases}$$

$$\mu = \begin{cases} \mu^- = 2 & \text{if } r \le R, \\ \mu^+ = 20 & \text{otherwise.} \end{cases}$$

The exact solution $u = (u_1, u_2)$ is:

$$u_1 = u_2 = \begin{cases} r^2 & \text{if } r \le R, \\ r^3 & \text{otherwise,} \end{cases}$$

where $r = \sqrt{x_1^2 + x_2^2}$. The exact solution has non-homogeneous jump conditions across Γ.

We show the grid refinement analysis in the infinity norm in Fig. 7. When coarser meshes (from a 20 by 20 mesh) are included, the average convergence order is 1.8541;

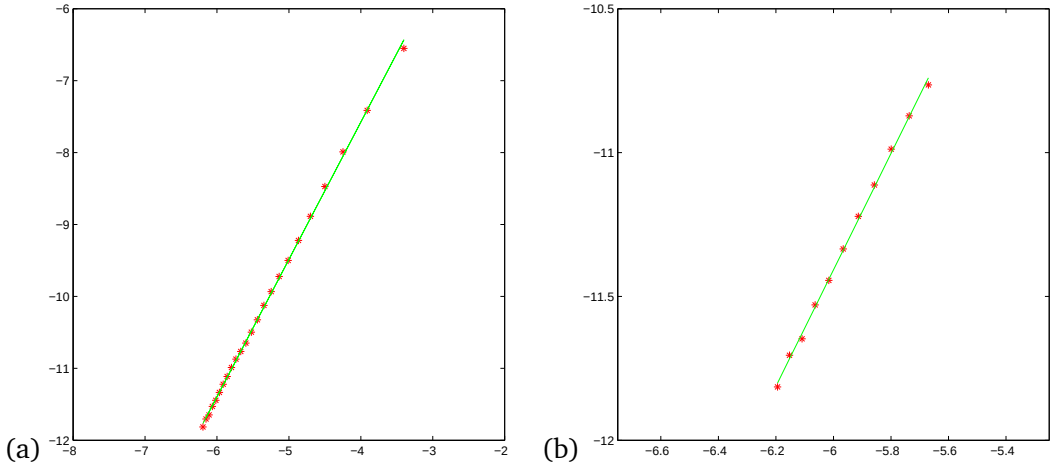

Figure 6: The linear regression analysis of $(u-u^h)$ in the L^∞ norm in log-log scale by using the conforming immersed interface finite element space and singularity removal technique. (a), the mesh varies according to $N = 20+20k$, $k = 0,1,\cdots,24$, the slope (convergence order) is 1.9095; (b), $N = 300+20k$, $k = 0,1,\cdots,10$, the slope is 2.0222.

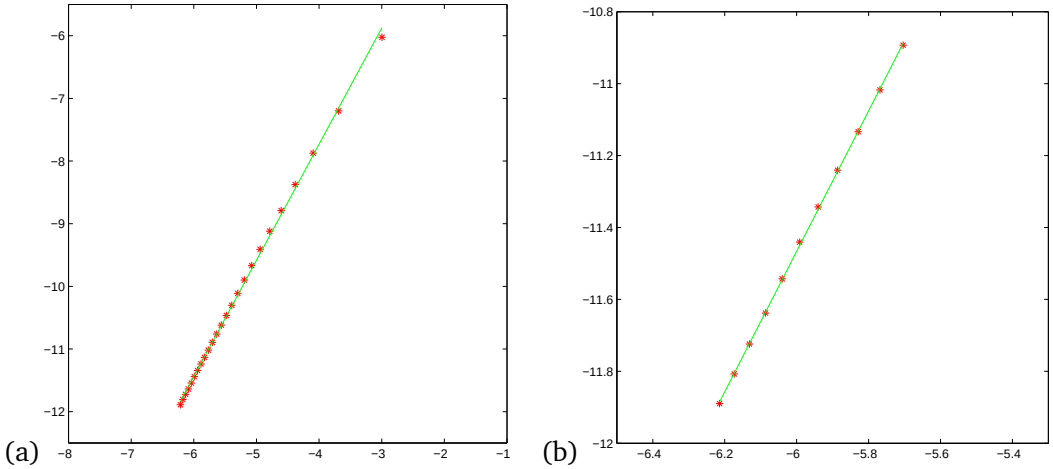

Figure 7: The linear regression analysis of $(u-u^h)$ in the L^∞ norm in log-log scale by using the conforming, linear, immersed interface finite element space. (a). the mesh is varying according to $N = 20+20k$, $k = 0,1,\cdots,24$, the slope (convergence order) is 1.8541; (b). $N = 300+20k$, $k = 0,1,\cdots,10$, the slope is 1.9519.

When finer meshes (from a 300 by 300 mesh) are included, the average convergence order is 1.9519. The results show that the new conforming immersed interface finite element method is second order accurate in the infinity norm for the elasticity problems with discontinuous Lamé constants and non-homogeneous jump conditions.

5. Conclusions

We have developed the immersed-interface finite-element methods for solving elasticity interface problems with *homogeneous and non-homogeneous jump conditions* using a uniform mesh. The described methods actually can be applied for any mesh. The interpolation function using the conforming finite element space is second order accurate. Numerical examples show that the developed methods have second order convergence rate in the L^∞ norm. The content of this paper is part of Y. Gong's PhD thesis [9].

Acknowledgments This work was partially supported by the US ARO grants 49308-MA and 56349-MA, the US AFSOR grant FA9550-06-1-024, the US NSF grant DMS-0911434, and the State Key Laboratory of Scientific and Engineering Computing of Chinese Academy of Sciences during a visit by Z. Li between July-August, 2008. We also like to thank Dr. Bo Li of University of California at San Diego for the original motivation, and many useful discussions and suggestions.

References

[1] I. Babuška. The finite element method for elliptic equations with discontinuous coefficients. *Computing*, 5:207–213, 1970.
[2] E. Bänsch, F. Haußer, O. Lakkis, B. Li, and A. Voigt. Finite element method for epitaxial growth with attachment-detachment kinetics. *J. Comput. Phys.*, 194:409–434, 2004.
[3] E. B. Becker, G. F. Carey, and J. T. Oden. *Finite Elements: An Introduction*. Prentice Hall, 1981.
[4] D. Braess. *Finite Elements*. Cambridge University Press, 1997.
[5] J. Bramble and J. King. A finite element method for interface problems in domains with smooth boundaries and interfaces. *Advances in Comput. Math.*, 6:109–138, 1996.
[6] W. K. Burton, N. Cabrera, and F. C. Frank. The growth of crystals and the equilibrium of their surfaces. *Phil. Trans. Roy. Soc. London Ser. A*, 243(866):299–358, 1951.
[7] K. Chan, K. Zhang, X. Liao, J. Zou, and G. Schubert. A three-dimensional spherical nonlinear interface dynamo. *The Astrophysical Journal*, 596:663–679, 2003.
[8] Z. Chen and J. Zou. Finite element methods and their convergence for elliptic and parabolic interface problems. *Numer. Math.*, 79:175–202, 1998.
[9] Y. Gong. Immersed-interface finite-element methods for elliptic and elasticity interface problems. PhD thesis, North Carolina State University, 2007.
[10] Y. Gong, B. Li, and Z. Li. Immersed-interface finite-element methods for elliptic interface problems with non-homogeneous jump conditions. *SIAM J. Numer. Anal.*, 46:472–495, 2008.
[11] H. Han. The numerical solutions of the interface problems by infinite element methods. *Numer. Math.*, 39:39–50, 1982.
[12] Z. Li. A fast iterative algorithm for elliptic interface problems. *SIAM J. Numer. Anal.*, 35:230–254, 1998.
[13] Z. Li and K. Ito. *The Immersed Interface Method – Numerical Solutions of PDEs Involving Interfaces and Irregular Domains*. SIAM Frontier Series in Applied mathematics, FR33, 2006.
[14] Z. Li, T. Lin, and X. Wu. New Cartesian grid methods for interface problem using finite element formulation. *Numer. Math.*, 96:61–98, 2003.
[15] S. Osher and R. Fedkiw. *Level Set Methods and Dynamic Implicit Surfaces*. Springer, New York, 2002.

[16] J. A. Sethian. *Level Set Methods and Fast Marching Methods*. Cambridge University Press, 2nd edition, 1999.

[17] J. Xu. Error estimates of the finite element method for the 2nd order elliptic equations with discontinuous coefficients. *J. Xiangtan University*, No. 1:1–5, 1982.

[18] X. Yang. Immersed interface method for elasticity problems with interfaces. PhD thesis, North Carolina State University, 2004.

[19] X. Yang, B. Li, and Z. Li. The immersed interface method for elasticity problems with interface. *Dynamics of Continuous, Discrete and Impulsive Systems.*, 10:783–808, 2003.